LM890828-1FR

LABORATORY MEMORANDUM NO. 110, 1989
LM890828-1FR
August 28, 1989

For circulation only within
Mobil Research and Development Corporation

DALLAS RESEARCH LABORATORY
Dallas, Texas

GEOSCIENCE RESEARCH
& TECHNICAL SERVICE
PROJECT No. 507-962
CC962

NUMERICAL SIMULATION OF LOW FREQUENCY ELECTRIC CURRENT FLOW IN ROCKS WITH APPLICATIONS TO FORMATION EVALUATION: AN APPLICATION OF THE CONNECTION MACHINE 2

17pg
Fig-5
Ref-1

Abstract

A numerical modeling technique applicable to the electrical behavior of complicated pore systems is described. Testing of the technique in two-dimensional models is complete, and three-dimensional codes developed to run on the DRL Connection Machine are under evaluation. Preliminary application to two-dimensional rocks have led to improved understanding of formation factor-porosity relations in rocks having secondary porosity.

Authors: W. D. Kennedy
D. C. Herrick
J. A. Pita

NOTICE

The data contained in this Memorandum are the responsibility of the authors and are unedited by DRL management. However, the Memorandum may contain confidential or proprietary information.

clt

Numerical Simulation of Low Frequency Electric Current Flow in Rocks with Applications to Formation Evaluation: An Application of the Connection Machine 2

INTRODUCTION

G. E. Archie (1942) described the relationship of formation resistivity factor to porosity and bulk resistivity to formation factor and water saturation. Archie's conclusions are based on empirical studies using rocks having primarily intergranular porosity. For simple packings of spherical grains, Archie's relations may be verified analytically; the relations may also be derived from certain regular analytical models which, however, are not very rock-like. When considering rocks of arbitrarily complicated grain shape, structure, packing, and conductivity, obtaining analytical forms for saturation equations from first principles is probably not possible, and empirical methods must still be employed. A difficulty with physical models having the features of real rocks of interest is that they are hard to construct and impossible to modify. The approach described herein replaces the physical model with a numerical model. The current distribution arising in the model resulting from applied potentials enable the calculation of the bulk resistivity R_o. Since R_w and porosity are parameters of the model, formation resistivity factor F may be calculated, and the relation between F and porosity studied. Techniques for constructing the numerical models are the subject of this discussion; interpretation of model studies are discussed in Herrick and Kennedy (1989).

Using the numerical model, such parameters as grain conductivity (including conductive coatings), microporosity, grain shape, pore throat dimension, and vug size, shape, and distribution may be varied more conveniently than in physical models. The same techniques can be applied to hydrocarbon-bearing rocks if the distribution of hydrocarbon within the pore system is known.

CONCLUSIONS

1. Finite difference modeling of the distribution of electric current in the pore structures of complicated rocks is a useful technique from which valuable insight into the behavior of actual rocks can be obtained.

2. The Connection Machine massively parallel computer makes possible higher resolution than would have been possible on a VAX because of the efficiency with which the solution to a given model can be obtained.

3. Improved understanding of the electrical behavior of complicated, non-Archie rocks has already been achieved in vuggy rocks (Herrick and Kennedy, 1989); application of the modeling technique implemented on the Connection Machine will make possible the study of other difficult-to-interpret resistivity problems.

PREVIOUS WORK

Aiken and others (1973) introduced the use of automated finite-difference resistivity modeling in geophysics. They developed a general theory and applied it to two-dimensional conductivity structures. Relaxation methods developed for use with hand calculators were implemented in FORTRAN and employed in the numerical solution to the field equations. Mufti (1976, 1978) formulated the two-dimensional problem using a non-uniform grid spacing and introduced successive overrelaxation as the solution technique. The problem was formulated for arbitrarily shaped three-dimensional conductivity structures by Dey and Morrison (1979). They extended the problem to three dimensions using a non-uniform grid spacing similar to Mufti's and formulated the problem in terms of matrix equations rather than grid operators. The matrix equation was efficiently solved on the sequential processors then available by means of a pre-conditioned conjugate gradient method using incomplete Cholesky factorization. Although the investigators cited above were interested in large-scale targets such as ore bodies or petroleum reservoirs, their techniques apply equally well to much smaller scales; in particular the three-dimensional finite difference technique can be applied to the study of electrical currents flowing in the pore spaces of rocks.

THEORY

Although the references cited contain the theoretical development required, it is convenient to recapitulate the theory below for completeness and in order to introduce the boundary condition employed in this work. The differential equation satisfied by the scalar electric potential can be obtained from the law of conservation of charge, Ohm's law, and the definition of the scalar potential. In differential form conservation of charge is expressed as

$$\nabla \cdot \mathbf{J} = -\frac{\partial \rho}{\partial t}\,\delta\,(x,y,z) \tag{1}$$

where **J** is current density (amperes/m^2), ρ is charge density (coulombs/m^3), and δ is a Dirac delta function representing the source. Ohm's law in field theory is expressed as

$$\mathbf{J} = \sigma\mathbf{E} \tag{2}$$

where σ is conductivity (siemens/m = mhos/m) and **E** is electric field intensity (volts/m). The electric field is related to a scalar electric potential, V, through

$$\mathbf{E} = -\nabla V. \tag{3}$$

Substituting (3) into (2) and the result into (1) yields

$$\nabla \cdot (-\sigma\nabla V) = -\frac{\partial \rho}{\partial t}\,\delta\,(x,y,z)\,. \tag{4}$$

Expansion of the left side of (4) by vector identities yields

$$\nabla\sigma\nabla V + \sigma\nabla^2 V = -\frac{\partial \rho}{\partial t}\,\delta\,(x,y,z)\,. \tag{5}$$

The left side is brought to a more conventient form by noting that

$$\nabla^2(\sigma V) = 2\nabla\sigma\nabla V + \sigma\nabla^2 V + V\nabla^2\sigma\,. \tag{6}$$

Substitution of (6) into (5) gives the result

$$\nabla^2(\sigma V) + \sigma\nabla^2 V - V\nabla^2\sigma = -2\,\frac{\partial \rho}{\partial t}\,\delta\,(x,y,z)\,. \tag{7}$$

Each term on the left is now expressed in terms of the same differential operator. The source term can be expressed in terms of current. Let $\rho = q/\Delta v$ where q is charge in coulombs and Δv is a volume element. Then $\partial\rho/\partial t = \partial q/\partial t/\Delta v = I/\Delta v$ where I is the net current entering or leaving the volume element. Except for volume elements containing current sources or sinks, $I = 0$; that is, all the current which enters the volume element also leaves it so there is no time dependent buildup of charge. In the models to be considered in this study the current sources are always considered to be remote from the model boundary. Thus equation (7) becomes

$$\nabla^2(\sigma V) + \sigma\nabla^2 V - V\nabla^2\sigma = 0. \tag{8}$$

BOUNDARY CONDITIONS

The spatial domain of the problem is a small rectangular prism containing a "numerical" sample of porous rock typifying the formation of interest. The region in the prism is discretized into a uniformly spaced three-dimensional mesh and the conductivity of the corresponding points in the sample are assigned to points in the numerical model. The fidelity of the numerical representation to the sample depends on the ratio of the size of the characteristic features in the sample and the grid interval. In order to obtain a tractable boundary condition, the sample is specially constructed so that its top and bottom and left and right boundaries conform to one another, i.e., if identical copies of the sample were stacked one-above-another, or laid side-by-side, grain boundaries in passing from one sample to another would be continuous. A more economical way to express this is to say that the sample is given periodic extensions in the $y-z$ plane. This periodicity permits "fictitious" points near, but outside, the sample to be represented by the corresponding points on the opposite side of, but interior to, the sample.

Although the current sources are outside the sample boundary, they are presumed to establish constant potentials on the front and rear faces of the sample. This amounts to choosing two boundary planes of the sample to lie on equipotentials of the current distribution actually flowing in the formation. Since the volume of the sample is small compared with the electrode or antenna arrays of logging sondes, and since the volume is taken to represent a sample relatively far from the well bore, the equipotentials should closely approximate parallel planes, and the choice of constant potentials on the front and back planes of the sample is justified.

COMPUTATION

Equation (8) was initially programmed in VAX FORTRAN using the method of successive overrelaxation (SOR) as described in *Numerical Recipes* (Press and others, 1986). Plans to implement a conjugate gradient algorithm on the VAX were changed when a Thinking Machines Corp. Connection Machine 2 (CM2) became available for DRL use. McDonald and Pita (1989) have shown that the conjugate gradient method maps very efficiently onto the CM2 architecture. The most time consuming computation in the conjugate gradient algorithm is a matrix-vector product that must be computed at each iteration. The matrix resulting from the finite-difference formulation with periodic boundary conditions is sparse, having 7 diagonals in two dimensions and 11 diagonals in three dimensions, all elements off these diagonals being equal to zero. For example, in the case of a 64 x 64 two-dimensional computational grid the coefficient matrix is 64^2 x 64^2 = 16,777,216 elements. Less than 20,480 of these elements, or only .1 percent, are non-zero. Thus storage of the entire matrix is not desirable. The diagonals can be stored in five 64 x 64 arrays called NORTH, SOUTH, EAST, WEST, and CENTER after their relative locations in the computational grid. The potential array also occupies a 64 x 64 array, V. The matrix-vector product is stored in a 64 x 64 array F. In FORTRAN 8X as implemented on the CM2, the matrix-vector multiplication is accomplished by

```
   F = NORTH*CSHIFT (V,DIM=1,SHIFT=-1) +
+      SOUTH*CSHIFT (V,DIM=1,SHIFT=1) +
+      WEST*EOSHIFT(V,DIM=2,SHIFT=1) +
+      EAST*EOSHIFT(V,DIM=2,SHIFT=-1) +
+      CENTER*V
```

where the CSHIFT intrinsic function of FORTRAN 8X implements the periodic boundary condition and the EOSHIFT introduces zero elements on the edges of the model where the potential is specified. It is interesting and instructive to see how the FORTRAN statement above accomplishes the matrix-vector multiplication. Consider a model of uniform conductivity = 1 s/m having 4 x 4 nodes at which the solution to Laplace's equation is known to equal 1 volt. The corresponding coefficient matrix is 16 x 16, and the matrix-vector multiplication is indicated by

$$\begin{bmatrix}
-4 & 1 & & & 1 & & & & & & & 1 & & & \\
1 & -4 & 1 & & & 1 & & & & & & & 1 & & \\
 & 1 & -4 & 1 & & & 1 & & & & & & & 1 & \\
 & & 1 & -4 & & & & 1 & & & & & & & 1 \\
 & & & & -4 & 1 & & & 1 & & & & & & \\
 & & & & 1 & -4 & 1 & & & 1 & & & & & \\
 & & & & & 1 & -4 & 1 & & & 1 & & & & \\
 & & & & & & 1 & -4 & & & & 1 & & & \\
 & & & & & & & & -4 & 1 & & & 1 & & \\
 & & & & & & & & 1 & -4 & 1 & & & 1 & \\
 & & & & & & & & & 1 & -4 & 1 & & & 1 \\
 & & & & & & & & & & 1 & -4 & & & 1 \\
1 & & & & & & & & & & & & -4 & 1 & \\
 & 1 & & & & & & & & & & & 1 & -4 & 1 \\
 & & 1 & & & & & & & & & & & 1 & -4 \\
 & & & 1 & & & & & & & & & & & 1
\end{bmatrix}
\begin{bmatrix} 1 \\ 1 \\ 1 \\ 1 \\ 1 \\ 1 \\ 1 \\ 1 \\ 1 \\ 1 \\ 1 \\ 1 \\ 1 \\ 1 \\ 1 \\ 1 \end{bmatrix}
=
\begin{bmatrix} -1 \\ 0 \\ 0 \\ -1 \\ -1 \\ 0 \\ 0 \\ -1 \\ -1 \\ 0 \\ 0 \\ -1 \\ -1 \\ 0 \\ 0 \\ -1 \end{bmatrix}$$

where the unfilled elements are equal to zero. Now note the addition of the 4 x 4 matrices

$$\begin{bmatrix} 1 & 1 & 1 & 1 \\ 1 & 1 & 1 & 1 \\ 1 & 1 & 1 & 1 \\ 1 & 1 & 1 & 1 \end{bmatrix} + \begin{bmatrix} 1 & 1 & 1 & 1 \\ 1 & 1 & 1 & 1 \\ 1 & 1 & 1 & 1 \\ 1 & 1 & 1 & 1 \end{bmatrix} + \begin{bmatrix} 0 & 1 & 1 & 1 \\ 0 & 1 & 1 & 1 \\ 0 & 1 & 1 & 1 \\ 0 & 1 & 1 & 1 \end{bmatrix} + \begin{bmatrix} 1 & 1 & 1 & 0 \\ 1 & 1 & 1 & 0 \\ 1 & 1 & 1 & 0 \\ 1 & 1 & 1 & 0 \end{bmatrix} +$$

$$\begin{bmatrix} -4 & -4 & -4 & -4 \\ -4 & -4 & -4 & -4 \\ -4 & -4 & -4 & -4 \\ -4 & -4 & -4 & -4 \end{bmatrix} = \begin{bmatrix} -1 & 0 & 0 & -1 \\ -1 & 0 & 0 & -1 \\ -1 & 0 & 0 & -1 \\ -1 & 0 & 0 & -1 \end{bmatrix}$$

Each matrix corresponds to one term in the FORTRAN assignment. The first pair of matricies on the left correspond to the CSHIFT functions in the FORTRAN assignment statement, while the second pair correspond to the EOSHIFT functions. (The CSHIFT results are the same since all the elements of $V = 1$; however, the algorithm remains valid for any matrix, V.)

If a column vector is formed from the transpose of the rows of the right side of this matrix equation, the result is the same as for the matrix multiplication above. Although this illustration is for the particular case NORTH = SOUTH = EAST = WEST = 1, CENTER = −4 and the vector $V = 1$, the result holds for any values of NORTH, SOUTH, EAST, WEST, CENTER, and V.

A two-dimensional conjugate gradient solution of equation (8) has been implemented on the CM2 and the results verified by comparison with SOR results obtained on a VAX.

To compare the performance of the a VAX and a CM2 a test problem was constructed. An infinite conductive cylinder embedded in a conductive whole space was represented on a 32 x 32 grid. The cylinder was assigned a radius of 10 grid intervals and a conductivity of 1 sieman/meter. The whole space was assigned a conductivity of .01 siemans/meter. This problem was run on a VAX 11/785 and a CM2. SOR was used on the VAX, while the conjugate gradient method was used on the CM2. Because different methods of solution were employed on the different machines, a comparison of the improvement in solution speed is not a direct measure of hardware improvement, some of the improvement being due to the more efficient solution. The comparison is, nonetheless, interesting. The VAX required 691 CPU seconds for 15000 iterations through the grid. The operation rate was approximately .2 megaflops (millions of *fl*oating point *op*erations per second). The CM2 required 345 iterations of an unpreconditioned and unoptimized conjugate gradient algorithm to obtain a comparable (or perhaps better) solution, attaining a rate of 5.28 megaflops in an elapsed time of about 6.5 seconds. Preconditioning the conjugate gradient matrix and optimizing the code would improve the operation rate; however, the factor of near 100 reduction in the time required to obtain a solution without these steps indicates the power of the CM2 for this class of problem. Moreover, for larger problems the rate of computation on the VAX remains fixed while the rate on the CM2 would increase until the number of nodes in the grid exceeds the number of physical processors in the CM2. Pita and McDonald (1989) report computation rates many times higher than reported here for large preconditioned conjugated gradient solutions.

Use of the CM2 coupled with the techniques of Pita and McDonald (1989) will make possible the investigation of more detailed three-dimensional models than would have been practical otherwise.

RESULTS

While three-dimensional studies using the CM2 have recently commenced, results for two dimensions, generated on a VAX, are complete. Figure 1 illustrates the results of the computation in a typical model. 51 x 51 nodes were used to represent a two-dimensional rock. The rock contains 4 grains distributed in a hexagonal close packed arrangement. This configuration was chosen because it represents a unit cell which can be replicated to form a larger structure. The grains, indicated by the circles and circular segments, are not allowed to touch in two dimensions because this would close the pore throats, thereby reducing the conductivity to zero. The grains were assigned a conductivity of $1. \times 10^{-13}$ s/m, and the regions between the grains were assigned a conductivity of 1 s/m in this model, although any desired conductivity can be assigned to any region. Potentials of +1 volts and −1 volts were applied at the top and bottom of the model, respectively. The stippled patterns show the potential distribution calculated from the finite difference model. Boundaries between the the stippled patterns correspond to equipotential contours. In regions where the conductivity is non-zero, the direction of current density is down the gradient of the potential or perpendicular to the equipotential lines.

Eight current streamlines are shown connecting the top and bottom of the model. These streamlines are boundaries of regions of constant current, i.e., no current crosses a streamline. Streamline plots thus give a qualitative understanding of the role of current stagnation zones which can occur in some models. A very important use of this and similar models is the computation of the total current flowing as the result of the applied potential. This allows the calculation of a value of R_0 and formation resistivity factor F for the model .

The equipotentials in the figure are not perfectly symmetric because the solution had not fully converged in this model. It was found in practice when using successive overrelaxation that one-fifth the number of iterations required to converge to visual symmetry produced adequate estimates of current; thus to minimize computational charges, most models generated were not allowed to converge fully.

A study of vuggy two-dimensional "rocks" using the techniques described above resulting in an improved understanding of formation resistivity factor - porosity relationships in these rock models has been completed (Herrick and Kennedy, 1989).

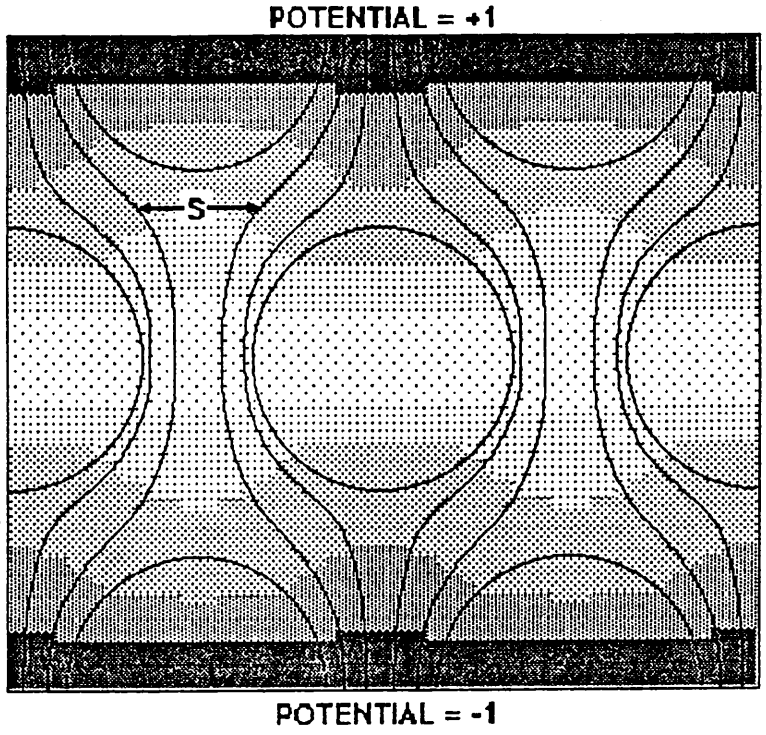

Figure 1. Potential distribution (stippled patterns) and current streamlines (S) in a finite difference model of idealized rock obtained by the method of successive overrelaxation.

REFERENCES

Aiken, C. L. V., D. A. Hastings, J. A. Sturgul, 1973, Physical and computer modeling of induced polarization, *Geophysical Prospecting* **21**, 763-782.

Archie, G. E., 1942, The Electrical Resistivity Log as an Aid in Determining Some Reservoir Characteristics, *Pet. Tech*, T.P. 1422, pp 1-8, Jan. 1942.

Dey, A., H. F. Morrison, 1979, Resistivity modeling for arbitrarily shaped three-dimensional structures, *Geophysics* **44**, 753-780.

Herrick, D. C., W. D. Kennedy, 1989, Numerical Modeling of the Electrical Properties of Non-Archie Rocks: Application to Formation Factor-Porosity Relationships of Two-Dimensional Pore Geometries, Lab. Memo. (in preparation).

McDonald, A. E., J. A. Pita, 1989, Connection Machine Performance on Typical Simulation Kernels, LM890601-1FR, Lab. Memo. No. 66, Mobil Res. and Dev. Corp.

Mufti, Irshad A., 1976, Finite-difference resistivity modeling for arbitrarily shaped two-dimensional structures, *Geophysics* **41**, 62-78.

Mufti, Irshad A., 1978, A practical approach to finite-difference resistivity modeling, *Geophysics* **43**, 930-942.

Pita, J. A., McDonald, A. E., 1989, Performance of a Family of Linear Solvers on the Connection Machine, LM890721-1FR, Lab. Memo. No. 91, Mobil Res. and Dev. Corp.

Press, W.H., B. P. Flannery, S. A. Teukolsky, W. T. Vetterling, 1986, *Numerical Recipes: The Art of Scientific Computing*, Cambridge University Press.

Pugh, E. M. Pugh, E. W., 1960, *Principles of Electricity and Magnetism*, Addison-Wesley Publishing Company, Inc.

Appendix

Comparison of Exact and Numerical Solutions

The number of boundary value problems for which exact, closed form solutions can be obtained is small; this is the impetus for development of numerical solution techniques. However, the numerical techniques require validation. In the case of Laplace's equation an analytical solution corresponding to the potential of an infinite conducting circular cylinder immersed in a conducting whole space permeated by a uniform field is easy to obtain. The results can then be compared to the numerical solution of the same problem.

Consider an infinite conducting cylinder embedded in an infinite conducting whole space. A uniform electric field $\mathbf{E} = E_0\hat{\mathbf{x}}$ exists everywhere in space. The governing differential equation is $\nabla \cdot \mathbf{J} = 0$. The constitutive relation $\mathbf{J} = \sigma\mathbf{E}$ is used to obtain

$$\nabla \cdot \sigma\mathbf{E} = -\nabla \cdot \sigma\nabla V = -\nabla\sigma\nabla V - \sigma\nabla^2 V = 0.$$

Thus away from the boundaries (where $\sigma\nabla = 0$), Laplace's equation $\nabla V^2 = 0$ holds. At the boundaries several conditions hold from which appropriate boundary conditions can be obtained:

1. The normal component of current density is continuous.
2. The tangential component of electric field is continuous.
3. In the far field the influence of the cylinder will vanish.

From the first condition we obtain

$$\mathbf{J}_1 \cdot \mathbf{r} = \mathbf{J}_2 \cdot \mathbf{r},$$
$$\Rightarrow \sigma_1\mathbf{E}_1 \cdot \mathbf{r} = \sigma_2\,\mathbf{E}_2 \cdot \mathbf{r},$$
$$\Rightarrow \sigma_1\,(\nabla V_1)_r = \sigma_2\,(\nabla V_2)_r,$$

leading at last to the useful boundary condition:

$$\sigma_1 \frac{\partial V_1}{\partial r}\Big|_a = \sigma_2 \frac{\partial V_2}{\partial r}\Big|_a.$$

From the second condition it is found that the potential itself is continuous, thus

$$V_1 \Big|_a = V_2 \Big|_a .$$

Finally, the field is constant for $r >> a \Rightarrow V = xE_0\hat{x} = r\cos\phi E_0\hat{x}$. From the general solution of the infinite cylinder in a uniform field, the potential can be shown to be of the form (Pugh and Pugh, 1960)

$$V_0 = Ar\ \cos\phi + \frac{B}{r}\cos\phi$$

outside the cylinder and

$$V_i = Cr\cos\phi$$

inside the cylinder. From the condition that the influence of the cylinder vanish at infinity we have

$$A = -E_0 \ .$$

The conditions that normal component of current density be continuous and tangential component of electric field be continuous give two equations for the coefficients B and C. The results are

$$B = E_0 a^2 \frac{\sigma_2 - \sigma_1}{\sigma_2 + \sigma_1} ,$$

$$C = E_0 \frac{2\sigma_1}{\sigma_2 + \sigma_1} .$$

Thus,

$$V_0 = E_0 r\cos\phi \left(1 - \left(\frac{a}{r}\right)^2 \frac{\sigma_2 - \sigma_1}{\sigma_2 + \sigma_1}\right)$$

and

$$V_i = E_0 r\cos\phi \ \frac{2\ \sigma_1}{\sigma_2 + \sigma_1} \ .$$

These equations can be used to compute the exact theoretical result for the potential of an infinite conducting cylinder in a uniform static field. The theoretical solution can be used to obtain potentials that exist at points corresponding to the nodes of a finite difference grid. The theoretical solution at nodes on the edges of the grid can be input as a fixed boundary potential to a numerical solution of the same problem. The potentials computed numerically are then compared with the analytical model potentials at the node locations to evaluate the quality of the numerical

Numerical Test

For test purposes a conductive cylinder of radius 10 and conductivity equal to 1 siemens/meter (1Ωm) was immersed in a resistive whole space of conductivity equal to .01 siemen/meter (100Ωm). The potential was sampled at an interval of .5 (arbitrary) distance units. The potential at the corners of a 66 x 64 grid was normalized to 1. The normalized potentials along the edges were then used at the boundaries of our numerical solution to compute a numerical solution at the remaining 64 x 62 interior nodes.

The results of the analytical calculation are shown by the plot in figure A1. Athough the plot represents the potentials due to a circular cylinder, the aspect ratio of characters on the line printer is about 1.6 to 1, causing circles to be represented as ellipses. The numbers occupying each node represent the absolute values of the potentials, multiplied by ten and truncated to integers. The results of the numerical solution give a very similar plot. To compare the analytical and numerical solutions, the absolute values of the differences of the two solutions at each were computed at each node, then multiplied by 100 and the results plotted and shown in figure A2. This presentation illustrates that the maximum difference in the solutions is about .05 near the edge of the cylinder. Away from the edges, the agreement is better than 1 part in 100. The reason for the poor result at the edge of the cylinder is that the finite difference approximation of the point derivatives is least accurate where the curvature of the field is greatest or when material boundaries are spanned by the finite difference operator. However, the numerical solution of the problem can be brought as close as desired to the analytical solution by selecting a fine enough grid interval. This and similar tests have been used to validate the numerical solutions obtained.

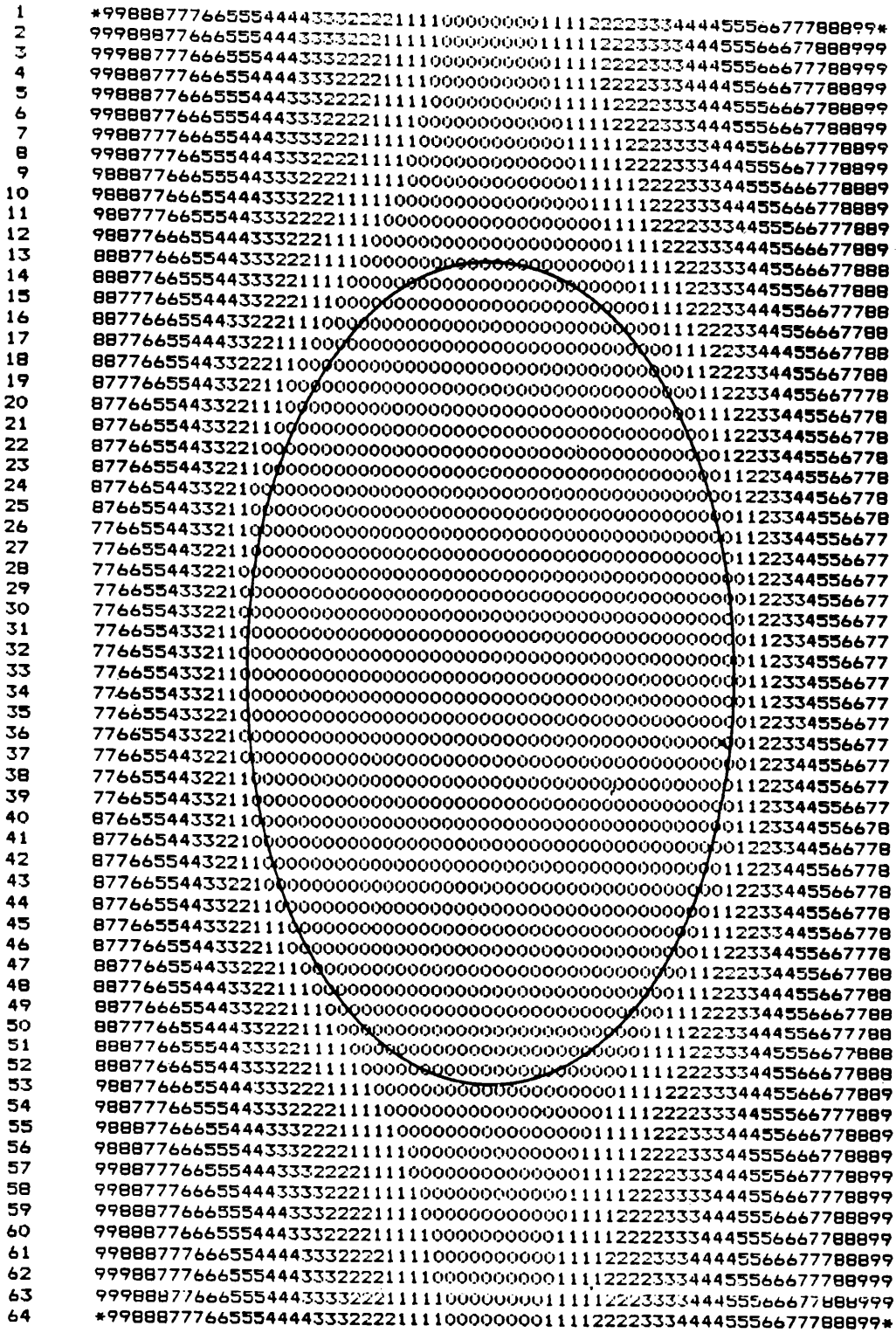

Figure A1. The theoretical potential distribution about a circular conductive cylinder immersed in a uniform field normal to the cylinder axis. The conductivity of the background medium is .01 s/m; the cylinder conductivity is 1 s/m. The potential is normalized to 1.0 at the corners of the figure; the absolute values multiplied by 10 and truncated are displayed by the printer. The circular geometry is distorted by the aspect ratio of the line printer. The numericall calculated potentials are quite similar.

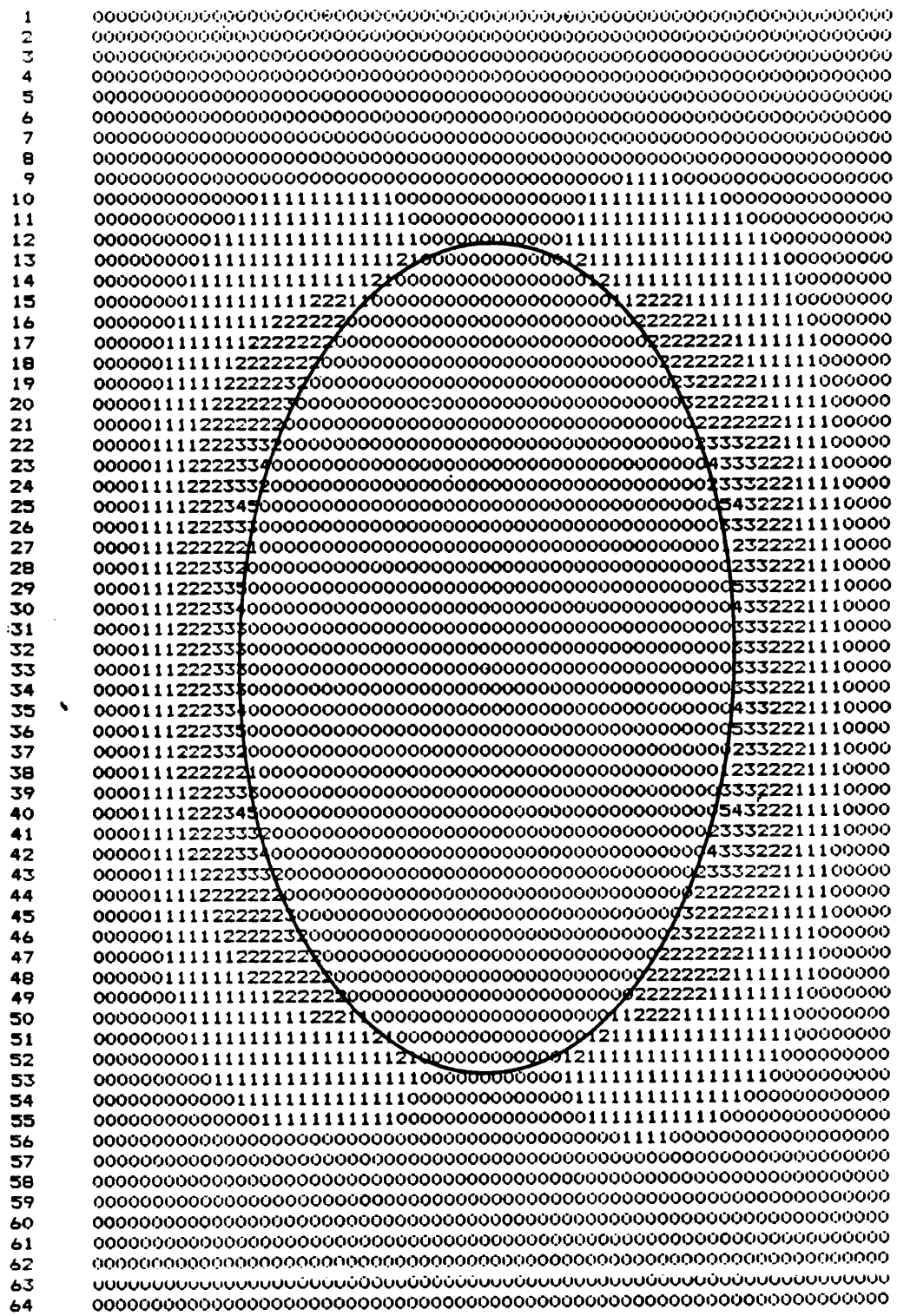

Figure A2. The difference between the exact analytical solution and the numerical solution is represented. The absolute values of the difference in the solutions are multiplied by 100 and truncated to produce the plot. The maximum difference is thus .05. The region where the greatest differences occur correspond to either regions where the curvature of the field is highest or a boundary of the cylinder is touched by the finite difference operator. In these regions the finite difference representation of ∇^2 is poorest.